Available online at www.sciencedirect.com
ScienceDirect
Mendeleev Commun., 2014, **24**, 360–362
Mendeleev Communications

Synthesis of SrF_2–YF_3 nanopowders by co-precipitation from aqueous solutions

Maria N. Mayakova,[a] Anna A. Luginina,[a] Sergey V. Kuznetsov,[a] Valerii V. Voronov,[a] Roman P. Ermakov,[a] Alexander E. Baranchikov,[b] Vladimir K. Ivanov,[b,c] Oksana V. Karban[d] and Pavel P. Fedorov*[a]

[a] *A. M. Prokhorov General Physics Institute, Russian Academy of Sciences, 119991 Moscow, Russian Federation. Fax: +7 499 135 7744; e-mail: ppfedorov@yandex.ru*
[b] *N. S. Kurnakov Institute of General and Inorganic Chemistry, Russian Academy of Sciences, 119991 Moscow, Russian Federation*
[c] *Department of Materials Science, M. V. Lomonosov Moscow State University, 119991 Moscow, Russian Federation*
[d] *Physical-Technical Institute, Ural Branch of the Russian Academy of Sciences, 426000 Izhevsk, Russian Federation*

DOI: 10.1016/j.mencom.2014.11.017

The $Sr_{1-x}Y_xF_{2+x}$ ($x \leqslant 0.6$) nanocrystalline solid solutions precipitated at an ambient temperature from the aqueous solutions of metal nitrates crystallized in a cubic system with $a = 5.800 - 0.230x$ [Å]; their composition range of homogeneity is wider than that for samples prepared at a higher temperature (from 850 °C to melt).

Nanocrystalline fluorides have been intensively studied[1–4] because of their applications as scintillators, acidic catalysts, cathode materials for alkaline batteries, thin antireflective coatings, drug components, precursors for laser and scintillation optical ceramics, *etc*. Strontium nanofluorides doped with rare earth ions can be used as promising luminophores.[5,6] They have been prepared by the thermolysis of metal trifluoroacetates, the microwaving of metal nitrates in 1-butyl-3-methylimidazolium tetrafluoroborate and hydrothermal techniques or obtained as nanocrystalline components of glass ceramics.[4,7–9] However, modern literature lacks information on the preparation of strontium rare-earth nanofluorides by co-precipitation from aqueous solutions. Recently, we found[4,6,7,10] that the latter approach is a very productive method for the preparation of equilibrium and non-equilibrium nanophases of variable composition formed under ambient conditions *via* a non-classical crystal growth mechanism (*i.e.*, by the oriented attachment of nanoparticles). Therefore, the goal of this study was to characterize nanopowders formed in the SrF_2–YF_3 model system during the precipitation of nanophases in aqueous solutions with hydrofluoric acid (HF).[†] The yttrium system was used as a model because it has similar physical and chemical properties to those of rare earth elements from Gd to Lu.

Chemical analysis and X-ray diffraction data for SrF_2–YF_3 samples, including pure SrF_2, are presented in Table 1 and Figure 1, respectively. They confirm a good agreement between the experimental and initial yttrium concentrations in the specimens.

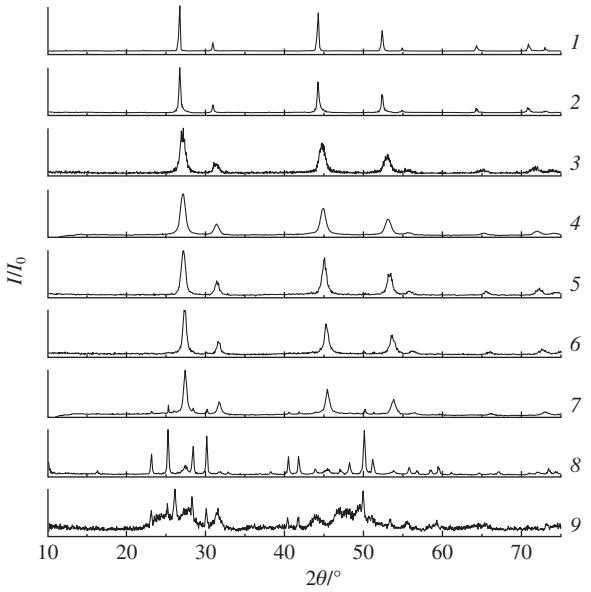

Figure 1 X-ray diffraction patterns of SrF_2–YF_3 samples precipitated from aqueous solutions, containing (*1*) 0, (*2*) 10, (*3*) 20, (*4*) 30, (*5*) 40, (*6*) 60, (*7*) 70, (*8*) 90 and (*9*) 100 mol% YF_3.

Samples with up to 60 mol% YF_3 displayed a single fluorite-type cubic phase (phase F). They also contained 2.5–4 wt% adsorbed water, which was removed after heating to 300 °C. This thermal treatment did not affect the unit cell parameters. Phase

[†] High-purity $Sr(NO_3)_2$ and $Y(NO_3)_3 \cdot 6H_2O$ (99.99%), HF (99.9%) and twice distilled water were used as starting materials. The precipitation experiments were carried out in polypropylene vessels at room temperature. The starting 0.17–0.20 M metal nitrate solutions were mixed in order to achieve Y/(Y + Sr) molar ratios from 10 to 90% and treated dropwise with aqueous HF (6 vol%) with vigorous stirring. The formed precipitates were decanted, thoroughly washed with twice distilled water and dried under air at 40 °C. In some experiments, pH of the mother solution was adjusted to 5–6.

The phase composition of the synthesized samples was controlled by X-ray diffraction analysis (DRON-4M diffractometer; CuKα radiation). The sizes of the domains of coherent scattering (DCS) and microdeformations were determined by a fundamental parameters technique[11] with the use of full profile analysis by the TOPAS software.[12]

Scanning electron microscopy (SEM) studies were carried out using a Carl Zeiss NVision 40 microscope, and atomic force microscopy (AFM) was performed with a Ntegra Prima scanning AFM probe.

The yttrium content in the prepared samples was determined by wet chemical analysis. A fluoride sample (~1 g) was placed in a glass-carbon dish and treated three times with sulfuric acid with complete evaporation after each treatment. Then, the residue was dissolved in 250 ml of water to completely transfer yttrium to the aqueous solution, whereas strontium remained in the undissolved precipitate. The resulting solution was titrated with a 0.1 M ethylenediaminetetraacetic acid (EDTA) solution at pH 5–6 and 50 °C. The equivalency point was determined by a change in the color of a xylenol orange indicator from red to yellow.

Table 1 Composition, crystal lattice parameters, values of the calculated sizes of the domains of coherent scattering D, and values of microdeformation e of the samples in SrF_2–YF_3 system.

Designated YF_3 content (mol%)	Experimental YF_3 content (wet chemical analysis data) (mol%)	Cubic crystal lattice parameter a/Å	D/nm	e
0	—	5.799±0.008	37±3	0.05±0.01
20	19±0.6	5.750±0.001	11±1	0.13±0.02
30	29±1.0	5.740±0.007	15±1	0.18±0.03
40	38±1.3	5.710±0.001	13±1	0.09±0.01
60	57±1.9	5.676±0.001	30±6	0.28±0.03

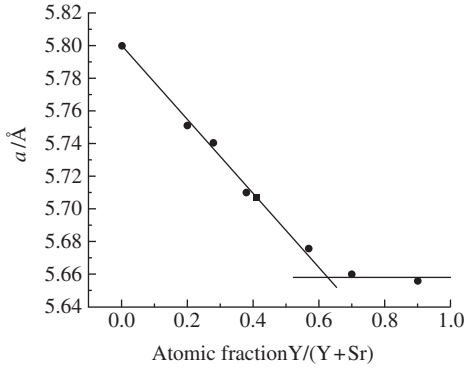

Figure 2 Parameters of the cubic crystal lattices of fluorite-type phases in the SrF_2–YF_3 system *vs.* the composition of samples prepared by high temperature synthesis[13] and precipitation from aqueous solutions.

F lattice parameter a varies from 5.799(8) Å for intrinsic SrF_2 (5.800 Å according to PCPDFWIN No. 060262) to 5.676(1) Å for $Sr_{1-x}Y_xF_{2+x}$ with x = 0.60, and it can be described with the following linear correlation: $a = 5.800 - 0.230x$ [Å], where x is the molar yttrium content in $Sr_{1-x}Y_xF_{2+x}$. This is consistent with data[13] for $Sr_{1-x}Y_xF_{2+x}$ ($x \leqslant 0.41$) (Figure 2). The latter fact is very important for practical purposes since it allows one to use known quantitative correlations for numerous SrF_2-based solid solutions of rare-earth fluorides[14] for the evaluation of the compositions of nanoparticles precipitated from aqueous solutions.

The scanning electron (SEM) and atomic force (AFM) microscopy images confirmed the hierarchic mechanisms of nanoparticle agglomeration. Thus, the SEM images of $Sr_{1-x}Y_xF_{2+x}$ specimens with x = 0.20 and 0.40 indicated the presence of ~20 nm nanoparticles [Figure 3(*a*),(*b*)]. This is in agreement with calculated D values (Table 1). The AFM data for the sample with x = 0.40 (Figure 4) show the formation of ~100 nm agglomerates.

Increasing the yttrium content of the specimens up to 70–90 mol% resulted in the formation of a second phase in the precipitates; in addition to the phase F with average a = 5.658(2) Å, one can observe another cubic phase, $(H_3O)Y_3F_{10}\cdot H_2O$,[10(*c*)] with the crystal lattice parameter a = 15.480(1) Å [*Fd*3*m* space group; $(H_3O)Yb_3F_{10}\cdot H_2O$ structure type[15]]. This phase contained hydroxonium ions; therefore, it can be represented as $(H_3O^+)Y_3F_{10}^-\cdot H_2O$. The two-phase composition of 90 mol% Y samples has also been confirmed by electron-microscopic data [Figure 3(*c*)]: the SEM images exhibit small 20 nm nanoparticles along with faceted octahedral ~200 nm $(H_3O)Y_3F_{10}\cdot H_2O$ nanocrystals, which are very similar to those observed earlier in the BaF_2–YF_3 system.[10(*c*)]

A comparison of the above results with known SrF_2–YF_3 phase diagram[16] (see Figure S1, Online Supplementary Materials) demonstrates that the composition area of the homogeneous fluorite-like cubic solid solution $Sr_{1-x}Y_xF_{2+x}$ (phase F) is wider for the precipitated samples (x = 0–0.60) than for the specimens prepared by high-temperature synthesis (x = 0–0.41). Additionally,

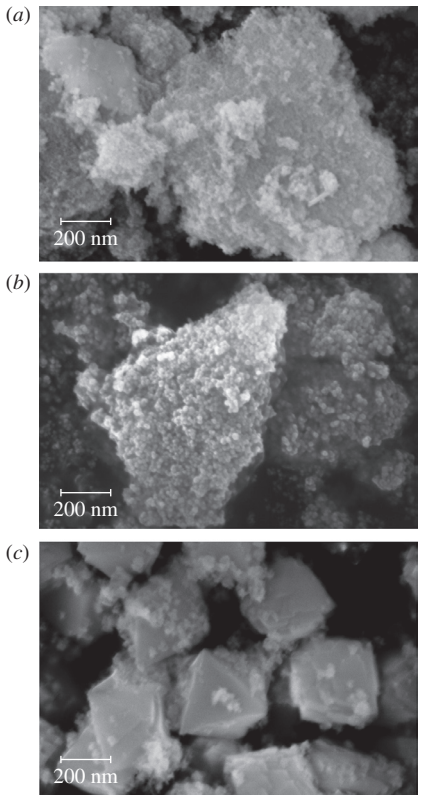

Figure 3 SEM images of (*a*) $0.8\,SrF_2$–$0.2\,YF_3$, (*b*) $0.6\,SrF_2$–$0.4\,YF_3$ and (*c*) $0.1\,SrF_2$–$0.9\,YF_3$ samples.

we did not observe the formation of a series of ordered fluorite-like phases at 33–44 mol% Y, which are thermodynamically stable at lower temperatures, as well as the formation of the high-temperature variable composition tysonite-type phase T.[16,17] One can assume that the boundary of the area of the phase F homogeneity is close to the spinodal border of the SrF_2–YF_3 system.[4,18]

The expansion of the area of homogeneity of the fluorite-type phase products prepared at an ambient temperature is very important for the synthesis of the new generation of solid electrolytes. The $Sr_{1-x}R_xF_{2+x}$ (R is a rare earth element) solid solutions possess high fluoride ionic conductivity which grows with the rare earth element (R) concentration.[19] Moreover, the nanoparticle character of such materials can seriously enhance the latter effect.[1,4]

Note that our experiments confirmed that the Sr:Y ratio in the starting solutions did not change during the precipitation of $Sr_{1-x}Y_xF_{2+x}$ nanopowders. This fact points to the congruent character of solid solution crystallization from aqueous solutions. This was also observed in CaF_2–RF_3 and BaF_2–RF_3 systems

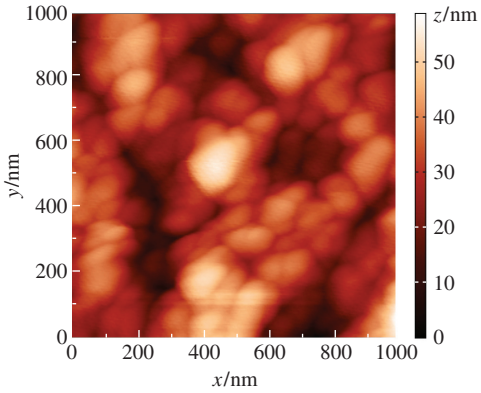

Figure 4 AFM image of the $0.6\,SrF_2$–$0.4\,YF_3$ sample.

convenient for the synthesis of optical material precursors.[6,7,10] Unfortunately, fluorite-type phases in $NaF–RF_3$ systems crystallize only incongruently from aqueous solutions.[10(*b*),(*d*)]

In conclusion, our experiments demonstrated that the treatment of $Sr(NO_3)_2$ and $Y(NO_3)_3$ with aqueous HF resulted in the precipitation of $Sr_{1-x}Y_xF_{2+x}$ nanopowder solid solutions. For $x \leqslant 0.6$, $Sr_{1-x}Y_xF_{2+x}$ specimens contained only one cubic phase with $a = 5.800 - 0.230x$ [Å]. If $x > 0.6$, the precipitates contained an additional cubic phase of $(H_3O)Y_3F_{10}·H_2O$.[15] In the precipitates, the Sr:Y molar ratio coincided with that for starting metal nitrate solutions. This fact confirmed the congruent character of $Sr_{1-x}Y_xF_{2+x}$ crystallization from aqueous media. The scanning electron and atomic force microscopy images of the synthesized nanoparticles justified the hierarchic mechanisms of their agglomeration.

We are grateful to R. Simoneaux, A. I. Popov and E. V. Chernova for their assistance in the preparation of this manuscript. This work was supported by the Russian Foundation for Basic Research (project no. 13-02-12162 ofi-m).

Online Supplementary Materials

Supplementary data associated with this article can be found in the online version at doi:10.1016/j.mencom.2014.11.017.

References

1 S. V. Kuznetzov, V. V. Osiko, E. A. Tkatchenko and P. P. Fedorov, *Russ. Chem. Rev*., 2006, **75**, 1065 (*Usp. Khim*., 2006, **75**, 1193).
2 *Fuctionalized Inorganic Fluorides: Synthesis, Characterization and Properties of Nanostructured Solids*, ed. A. Tressaud, John Wiley & Sons, Chichester, 2010.
3 M. Haase and H. Schafer, *Angew. Chem. Int. Ed.*, 2011, **50**, 5808.
4 P. P. Fedorov, A. A. Luginina, S. V. Kuznetsov and V. V. Osiko, *J. Fluorine Chem.*, 2011, **132**, 1012.
5 C. Cao, W. Qin, J. Zhang, Y. Wang, G. Wang, G. Wei, P. Zhu, L. Wang and L. Jin, *Opt. Commun.*, 2008, **281**, 1716.
6 Yu. A. Rozhnova, A. A. Luginina, V. V. Voronov, R. P. Ermakov, S. V. Kuznetsov, A. V. Ryabova, D. V. Pominova, V. V. Arbenina, V. V. Osiko and P. P. Fedorov, *Mat. Chem. Phys*., 2014, **148**, 201.
7 A. A. Luginina, P. P. Fedorov, S. V. Kuznetsov, M. N. Mayakova, V. V. Osiko, V. K. Ivanov and A. E. Baranchikov, *Inorg. Mater.*, 2012, **48**, 531 (*Neorg. Mater.*, 2012, **48**, 617).
8 J. Peng, S. Hou, X. Liu, J. Feng, X. Yu, Y. Xing and Z. Su, *Mater. Res. Bull*., 2012, **47**, 328.
9 X. S. Qiao, X. P. Fan, Z. Xue, X. H. Xu and O. Q. Lu, *J. Alloys Compd*., 2011, **509**, 4714.
10 (*a*) S. V. Kuznetsov, P. P. Fedorov, V. V. Voronov, K. S. Samarina, R. P. Ermakov and V. V. Osiko, *Russ. J. Inorg. Chem*., 2010, **55**, 484 (*Zh. Neorg. Khim*., 2010, **55**, 536); (*b*) P. P. Fedorov, S. V. Kuznetsov, M. N. Mayakova, V. V. Voronov, R. P. Ermakov, A. E. Baranchikov and V. V. Osiko, *Russ. J. Inorg. Chem*., 2011, **56**, 1525 (*Zh. Neorg. Khim*., 2011, **56**, 1604); (*c*) P. P. Fedorov, M. N. Mayakova, S. V. Kuznetsov, V. V. Voronov, R. P. Ermakov, K. S. Samarina, A. I. Popov and V. V. Osiko, *Mater. Res. Bull.*, 2012, **47**, 1794; (*d*) S. V. Kuznetsov, A. A. Ovsyannikova, E. A. Tupitsyna, D. S. Yasyrkina, V. V. Voronov, P. P. Fedorov, N. I. Batyrev, L. D. Iskhakova and V. V. Osiko, *J. Fluorine Chem*., 2014, **161**, 95; (*e*) P. P. Fedorov, V. V. Osiko, S. V. Kuznetsov, O. V. Uvarov, M. N. Mayakova, D. S. Yasirkina, A. A. Ovsyannikova, V. V. Voronov and V. K. Ivanov, *J. Cryst. Growth*, 2014, **401**, 63.
11 J. Bergmann, R. Kleeberg, A. Haase and B. Breidenstein, *Mater. Sci. Forum*, 2000, **347–349**, 303.
12 A. A. Coelho, J. S. O. Evans, I. R. Evans, A. Kern and S. Parsons, *Powder Diffr.*, 2011, **26**, 22.
13 B. P. Sobolev, K. B. Seiranian, L. S. Garashina and P. P. Fedorov, *J. Solid State Chem.*, 1979, **28**, 51.
14 P. P. Fedorov and B. P. Sobolev, *Sov. Phys. Crystallogr*., 1992, **37**, 651 (*Kristallografiya*, 1992, **37**, 1210).
15 F. Le Berre, E. Boucher, M. Allain and G. Courbion, *J. Mater. Chem*., 2000, **10**, 2578.
16 B. P. Sobolev and K. B. Seiranian, *J. Solid State Chem.*, 1981, **39**, 17.
17 B. P. Sobolev, V. B. Aleksandrov, P. P. Fedorov, K. B. Seiranyan and N. L. Tkachenko, *Sov. Phys. Crystallogr*., 1976, **21**, 49 (*Kristallografiya*, 1976, **21**, 96).
18 P. P. Fedorov, *Russ. J. Inorg. Chem.*, 2000, **45**, Suppl. 3, 268.
19 A. K. Ivanov-Shits, N. I. Sorokin, P. P. Fedorov and B. P. Sobolev, *Solid State Ionics*, 1989, **31**, 253.

Received: 24th March 2014; Com. 14/4330